PROCEEDINGS OF SPIE

SPIEDigitalLibrary.org/conference-proceedings-of-spie

# Holographic imaging and interferometry with non-Bragg diffraction orders in lithium niobate and photothermoplastic materials

Nickolai Kukhtarev, Tatiana Kukhtareva, Arcadi Chirita

Nickolai Kukhtarev, Tatiana Kukhtareva, Arcadi Chirita, "Holographic imaging and interferometry with non-Bragg diffraction orders in lithium niobate and photothermoplastic materials," Proc. SPIE 8497, Photonic Fiber and Crystal Devices: Advances in Materials and Innovations in Device Applications VI, 849706 (15 October 2012); doi: 10.1117/12.928543

SPIE.

Event: SPIE Optical Engineering + Applications, 2012, San Diego, California, United States

Downloaded From: https://www.spiedigitallibrary.org/conference-proceedings-of-spie on 28 Nov 2023 Terms of Use: https://www.spiedigitallibrary.org/terms-of-use

# Holographic imaging and interferometry with non-Bragg diffraction orders in lithium niobate and photo-thermoplastic materials

Nickolai Kukhtarev*, Tatiana Kukhtareva *, Arcadi Chirita**,
- Physics Department, Alabama A&M University, Huntsville AL 35762, USA
- ** Department of Physics, State University of Moldova, Moldova Republic

## ABSTRACT

We investigated recording of holographic volume and surface-relief gratings in photorefractive crystal and in a photo-thermoplastic (PTP) holographic camera. Holographic recording with an image-bearing signal beam leads to the appearance of two Bragg and two or more non-Bragg diffracted beams that shows the transformed images in each beam (rotation and angular amplification of images). Using this real-time mode of interferometry, the hologram is retrieved with a deformed object beam, resulting in the appearance of fringes with a proper phase shift in each of four diffracted beams. Retrieval with a time-modulated single-pixel object beam lead of time-modulated response in all diffraction orders. This one-shot (one-exposure) phase-shifting interferometry results in clarifying the object wave-front information (as an example, from the surface deformation) and solving the sign ambiguity problem. This procedure demonstrates that high-resolution holographic imaging of the PTP holographic camera static deformations in the order of ~0.1mm can be revealed on the diffusion reflection surface. In addition, it was demonstrated, that using the PTP materials could achieve holographic recording and imaging through phase aberration, with the image appearing in the non-Bragg diffraction order.

*Keywords: real-time holography, interferometry*

## 1. INTRODUCTION

In this paper, we considered the self-diffraction in volume gratings of lithium niobate crystals (LN), and analysed Bragg and first non-Bragg orders. Furthermore, we investigated the diffraction as seen on volume and surface-relief gratings in photo-thermoplastic (PTP) carriers. In the volume grating (LN) two types of interferometric beam coupling is seen, namely, self-diffraction and coherent beam combining.

Two-beam coupling in LN is a non-linear process [1], when two laser beams are employed to record holographic grating by modulating the refractive index, they simultaneously diffract on this grating, thus the term self-diffraction. We show that aside from the well-known effects of energy and phase transformation in the Bragg beams, first non-Bragg diffraction orders may appear even for thick volume gratings. It has been shown, that forward phase conjugation and phase doubling occur in non-Bragg orders [1]. However, we show that in coherent beam combining, all four beams (2 Bragg and 2 non-Bragg) are sensitive to the seeking phase modulation as well as to the type of non-linear process of grating recording.

In PTP self-diffraction is due to the formation of volume or surface phase-relief grating [2-4] that also produces efficient high-order diffraction beams. We will analyze the similarity through imaging and through holographic interferometry with higher diffraction orders for these two vastly different recording media. It is interesting to note that the similarity between the gratings with large amplitudes of surface relief and the volume grating was discussed in the paper [4]. In spite of the differences between lithium niobate and PTP n the mechanism of recording, both materials allow for the recording of efficient holograms with similarity in the transformation of images in non-Bragg orders.

Photonic Fiber and Crystal Devices: Advances in Materials and Innovations in Device Applications VI,
edited by Shizhuo Yin, Ruyan Guo, Proc. of SPIE Vol. 8497, 849706 · © 2012 SPIE
CCC code: 0277-786/12/$18 · doi: 10.1117/12.928543



Downloaded From: https://www.spiedigitallibrary.org/conference-proceedings-of-spie on 28 Nov 2023
Terms of Use: https://www.spiedigitallibrary.org/terms-of-use

Holographic recording results in structural transformations in the chalcogenide glassy semiconductor (CGS) layer, leading to changes in optical and electrical characteristics of the semiconductor.
The diffraction grating is recorded in such a way that it is stored as a "hidden" image in CGS layer. The "hidden" image, stored in the CGS layer, is finally transformed in the relief-phase grating in the thermoplastic layer [6].

The goal of the present work is to study the possibility of the application of the PTP films and lithium-niobate crystals in the recording of micro-object holograms for imaging and holographic interferometry, using non-Bragg diffraction orders.

## 2. THEORETICAL MODELING AND EXPERIMENTAL SETUP IN LN CRYSTAL

Real time holographic interferometry is applied for applications like non-destructive testing. In his method, the initial state of the object is holographically recorded as shown in Figure.1. During the recording of the grating in the photorefractive (PR) LN crystal, photo-induced changes of the refractive index develop in real time and recording beams (amplitudes, phases and polarizations) may also change by self-diffraction.

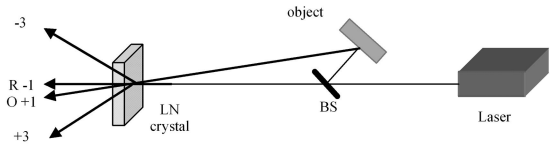



Figure 1. Schematic of the dynamic hologram recording in LN crystal (object O and reference R waves) with generation of the first non-Bragg orders (+3, -3)

In the symmetrical geometry, a laser wave time independent amplitude $F$ can be written as a Fourier decomposition of plane waves of the form [1]

$$F = \sum_{s=\pm1,\pm3} C_s e^{i(sk_x x - k_z z)}. \qquad (1)$$

For the symmetric geometry of recording shown in Figure 1, the coupled-wave equations for the complex amplitude of the recording waves are given by:

$$\frac{dC_{\pm1}}{dz} = iME_{\pm2}C_{\mp1}, \qquad \mathbf{(2)}$$

where, $i = \sqrt{-1}$, $z$ is the axial coordinate along the depth of the crystal, $M = \frac{rkn^3}{2\cos\theta}$, $r$ is an effective electro-optic coefficient of the LN crystal, $E_{\pm2}$ are components of the holographic electric-field grating, $k$ is wave number and $n$ is the refractive index. It is convenient to introduce refractive index grating with the amplitude

$$n_{\pm2} = \cos\vartheta ME_{\pm2}/k.$$



Downloaded From: https://www.spiedigitallibrary.org/conference-proceedings-of-spie on 28 Nov 2023
Terms of Use: https://www.spiedigitallibrary.org/terms-of-use

In further theorizing, we will consider the modulation of the refractive index **as** a phenomenological parameter. Thus, our approach can also be used as the description of the holographic recording of volume grating in PTP film, based on the photo-structural transformations.

Equations for the non-Bragg orders can be written as [1]

$$\frac{dC_{\pm 3}}{dz} - iqC_{\pm 3} = \frac{ikn_{\pm 2}C_{\pm 1}}{\cos\theta} \tag{3}$$

where $q = 4\frac{k_x^2}{k_z}$ is the geometric phase mismatch for the diffracted non-Bragg orders, .

For a local response, when only phase changes occur during recording, results may be written in the compact form. Denoting input amplitudes of the two reading waves (in real-time mode) $C_{\pm}(0) = A_{\pm}$.

We can write the intensities in the two Bragg and the two non-Bragg orders as:

$$V_{+1} = \left|C_{+1}\right|^2 = V_{+1,T} + V_{+1,D} + 2\sqrt{V_{+1,T}V_{+1,D}}\cos(\Phi + \Psi_{+1}) \tag{4a}$$

$$V_{-1} = \left|C_{-1}\right|^2 = V_{-1,T} + V_{-1,D} + 2\sqrt{V_{-1,T}V_{-1,D}}\cos(\Phi + \Psi_{-1}) \tag{4b}$$

For non-Bragg orders we can get:

$$V_{+3}(z) = \left|C_{+3}(z)\right|^2 = V_{+3,+} + V_{+3,-} + \sqrt{V_{+3,+}V_{+3,-}}\cos(\Phi + \Psi_{+3}) \tag{5a}$$

$$V_{-3}(z) = \left|C_{-3}(z)\right|^2 = V_{-3,-} + V_{-3,+} + \sqrt{V_{-3,-}V_{-3,+}}\cos(\Phi + \Psi_{-3}) \tag{5b}$$

where the values of $V_{+1,T}, V_{+1,D}, \Psi_{+1}, V_{-1,T}, V_{-1,D}, \Psi_{-1}, V_{+3,+}, V_{+3,-}, \Psi_{+3}, V_{-3,-}, V_{-3,+}, \Psi_{-3}$ are determined by the parameters of recording material or they may be found from the calibration experiment of an object that has a known phase modulation Φ.

For the lithium niobate crystal we can write in explicit form for Bragg orders:

$$V_{+1,T} = \left|A_{+_+}D_+\right|^2, V_{+1,D} = \left|A_-D_-\right|^2, \Phi = Arc(A_+A_-^*), \Psi_{+1} = Arc(D_+D_-^*)$$

$$V_{-1,T} = \left|A_-E_-\right|^2, V_{-1,D} = \left|A_+E_+\right|^2, \Psi_{-1} = Arc(E_+, E_-^*)$$

Here $D_+ = \frac{e^{-ix\beta}}{1+b}(be^{ix} + e^{-ix}), D_- = \frac{e^{-ix\beta}\sqrt{b}}{1+b}(e^{-ix} - e^{-ix})$

$$E_+ = \frac{e^{-2ix\beta}}{(1+b)\sqrt{b}}(be^{ix(1-\beta)} - e^{-ix(1+\beta)})$$

$$E_- = \frac{e^{-2ix\beta}\sqrt{b}}{(1+b)}(e^{ix(1-\beta)} + e^{-ix(1+\beta)}), x \equiv \frac{\gamma^2}{2}, \beta = \frac{\text{b - 1}}{\text{b + 1}}$$

For non-Bragg orders we can write



Downloaded From: https://www.spiedigitallibrary.org/conference-proceedings-of-spie on 28 Nov 2023
Terms of Use: https://www.spiedigitallibrary.org/terms-of-use

$$V_{+3}(z) = \left|C_{+3}(z)\right|^2 = V_{+3,+} + V_{+3,-} + \sqrt{V_{+3,+}}V_{+3-}\cos(\Phi + \Psi_{+3})$$

Here

$$V_{-3,\pm} = \left|A_{\pm}F_{\pm}\right|^2, F_{\pm} = \frac{i\gamma\sqrt{b}}{1+b}e^{iQz}\int_0^z e^{-iz'(\beta\gamma+Q)}D_{\pm}(z')dz'$$

$$\Psi_{+3} = Arc(F_{+}F_{-}^{*})$$

$$V_{-3}(z) = \left|C_{-3}(z)\right|^2 = V_{-3,-} + V_{-3,+} + \sqrt{V_{-3,-}}V_{-3+}\cos(\Phi + \Psi_{-3})$$

Here :

$$V_{-3,\pm} = \left|A_{\pm}G_{\pm}\right|^2, G_{\pm} = \frac{i\gamma\sqrt{b}}{(1+b)}e^{iQz}\int_0^z e^{iz'(\gamma\beta-Q)}E_{\pm}(z')dz'$$

$$\Psi_{-3} = Arc(G_{+}G_{-}^{*})$$

From Eqs. 4(a,b) and Eqs. 5(a,b), the intensities of the two Bragg and the two non-Bragg orders, all have phase change Φ with different phase shifts $\Psi_{\pm 1}, \Psi_{\pm 3}$. Thus, it means that during one shot (one exposure and conceptive reading) we have four equations for intensities that contain the phase Φ with different phase shifts.

### 2.1 Retrieval with phase modulation.

To describe retrieval with phase modulation, we have in general case to solve time- dependent equation for the refractive-index grating:

$$\frac{dn_{+2}}{dt} + \frac{n_{+2}}{\tau} = \frac{C_{+1}C^{*}{}_{-1}}{I_0\tau k}(i\Gamma\ /2 + \gamma)\cos\vartheta \qquad (6)$$

here $\tau$ is a relaxation time of grating recording.

General solution of equation (6) can be written in the integral form:

$$n_{+2}(t) = n_{+2}(0)e^{-t/\tau} + \int_0^t \frac{C_{+1}C^{*}{}_{-1}}{I_0\tau k}(i\ \Gamma/2 + \gamma)e^{i(t'-t)}dt'\cos\theta \qquad (7)$$

Where first term in the right-hand side of (7) describe decay of the old grating, and the second term show build-up of the new grating.

For very slow grating recording and erasure and for short observation time we may ignore time dependence of recorded grating and consider time modulation of phases parametrically.



Downloaded From: https://www.spiedigitallibrary.org/conference-proceedings-of-spie on 28 Nov 2023
Terms of Use: https://www.spiedigitallibrary.org/terms-of-use

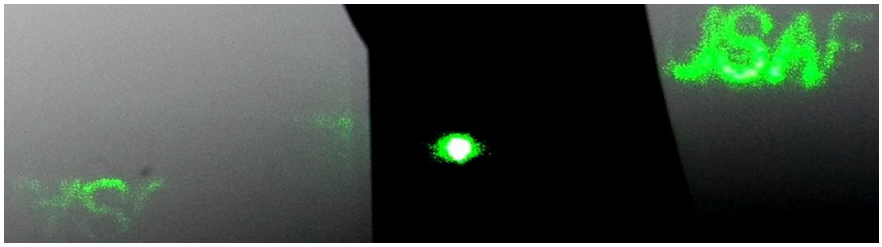


Fig.2. Imaging with non-Bragg order (left) that show rotation of image on the 180 degree along the direction of propagation (recording in the 2mm thick Lithium-Niobate crystal, cone angle about 2 degree). Object: reflection from the Air Force resolution chart.

In the Fig.2 it is shown images of reflection object (US Air-Force resolution chart) in phase-conjugated non-Bragg order (left) and in transmitted object beam (right) that are 180-degree rotated.

## 3. RECORDING IN PHOTO-THERMOPLASTIC CARRIERS

The recording of the surface relief phase grating in PTP film includes several stages that are described in the papers [2, 3].

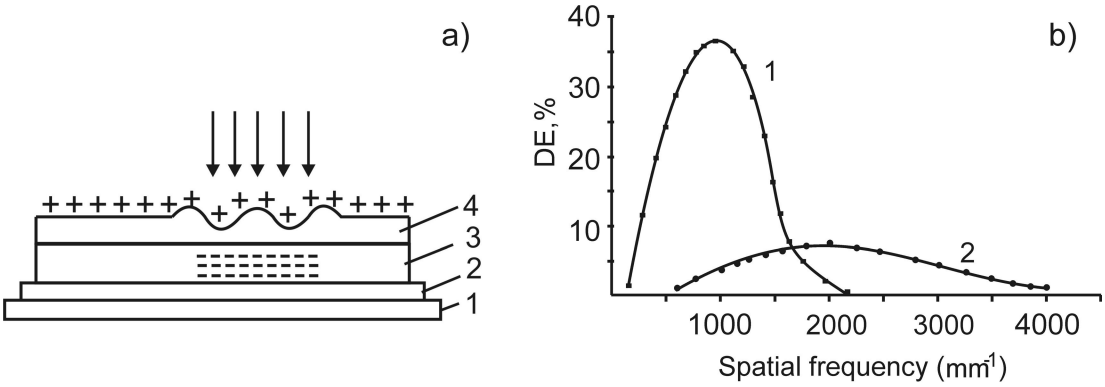



Figure 3. a) An illustration of the recording mechanism, b) The dependence of the diffraction efficiency on spatial frequency.

A transparent chrome electrode of (2) was deposited on the flexible polymer film (1). A layer of the chalcogenide glassy semiconductor As-Se-S (3) with thickness range of 0.2- 2.6 $\mu$m was deposited on top of the metal electrode. The thermoplastic layer (4) (thickness 0.2-0.7 $\mu$m) is based on the co-polymers and oligomers and was deposited from the solution of thermoplastic in toluene.

The maximum diffraction efficiency, resolution power and holographic sensitivity were registered for thermoplastic layer based on poly-N-epoxypropylcarbazole. Figure 3b shows the diffraction efficiency



Downloaded From: https://www.spiedigitallibrary.org/conference-proceedings-of-spie on 28 Nov 2023
Terms of Use: https://www.spiedigitallibrary.org/terms-of-use

dependence on spatial frequency for thermoplastic layer thickness 0.5 $\mu$m (1) and 0.2 $\mu$m (2). For PTP with thermoplastic thickness 0.5 $\mu$m, the diffraction efficiency of phase-relief grating was near 37% (curve 1, Figure 3b which was close to the maximum of 40% for phase-relief gratings [3].
Surface scanning using AFM of diffraction grating with spatial frequency 1000 $mm^{-1}$ (0.5 $\mu$m thermoplastic thickness) reveals (Figure 4a) that the sinusoidal profile of the grating has a high depth of modulation of 0.42 that allows getting the high diffraction efficiency[6]

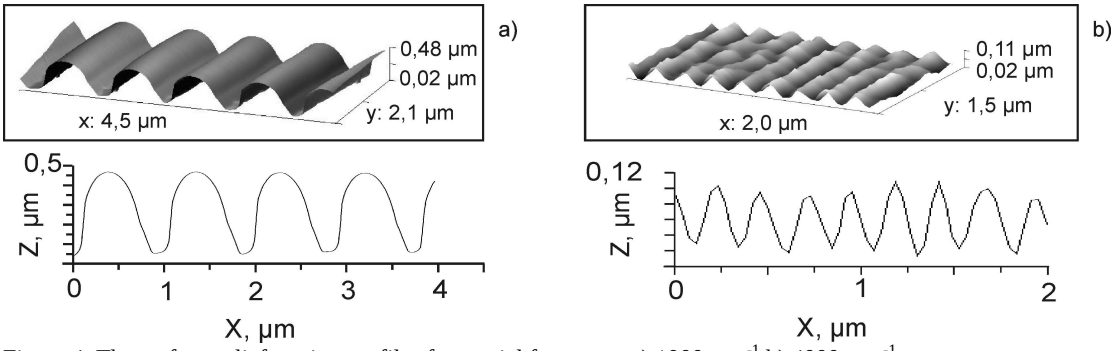


Figure 4. The surface-relief grating profiles for spatial frequency a) 1000 $mm^{-1}$ b) 4000 $mm^{-1}$

On the PTP with 0.2 $\mu$m thermoplastic thickness the grating registered with a high spatial frequency of 4000 $mm^{-1}$ with 0,5% diffraction efficiency (DE) (curve 2, Figure 3b). A high spatial resolution is achieved for the thin thermoplastic layers with relatively low depth of modulation of 0,09 microns (Figure 4b) but in this case a diffraction efficiency decreases. The threshold holographic sensitivity for PTP carriers based on 68mol%$As_4S_3Se_3$ -28mol%$As_2S_3$ system with a thermoplastic layer of poly-N -epoxypropylcarbasole for coherent radiation on 532 nm is S=5x$10^6$$cm^2$/J with DE=1%.

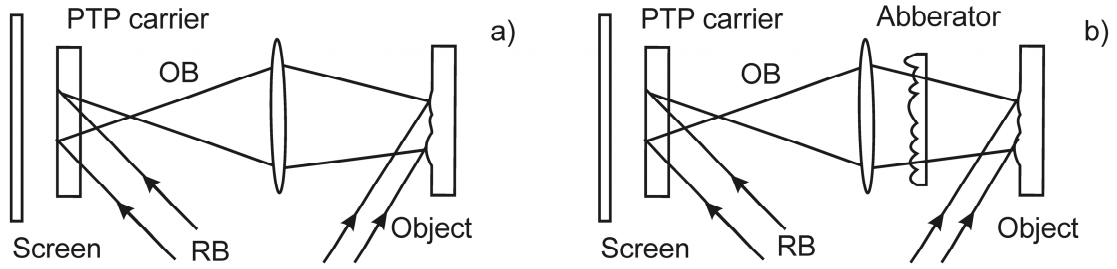


Figure 5. The schematic of holographic recording of: a) holographic interferometry, b) holographic imaging via an aberrator

Real-time interferometry was demonstrated using the recording by green laser (532 nm) as shown in the Figure 5a. Non-transparent letters LA placed on the Si single crystal plate was used as the object. The initial stage recording is shown on the Figure 6.



Downloaded From: https://www.spiedigitallibrary.org/conference-proceedings-of-spie on 28 Nov 2023
Terms of Use: https://www.spiedigitallibrary.org/terms-of-use

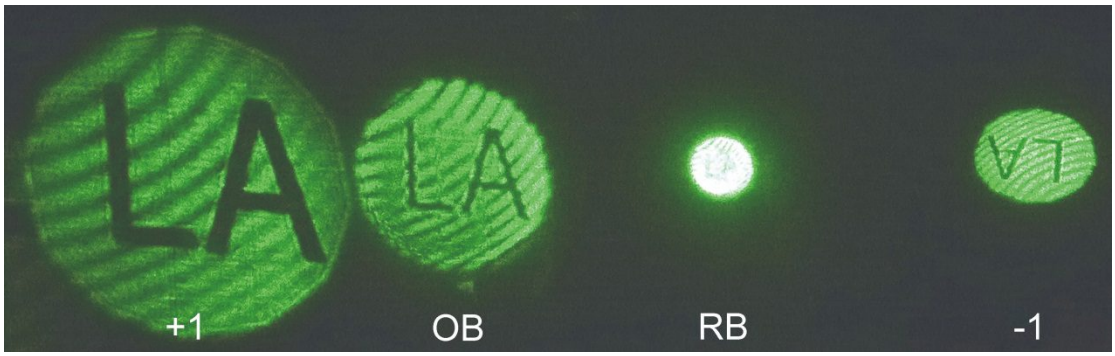
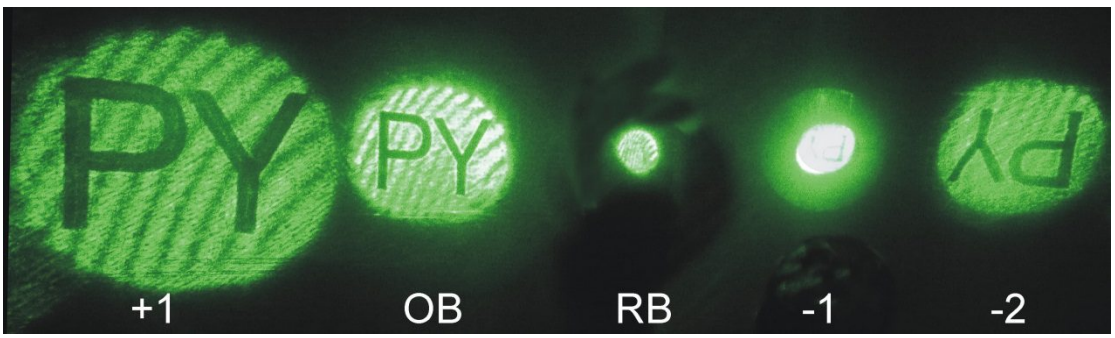



Figure 6. Real-time recording of the object initial state

In the reconstructed image (Figure 6) there are images in Bragg and in non-Bragg orders, with the rotated image in the (+1) order, which is similar to what was observed in the similar experiment on lithium - niobate crystal (see Figure 2). The explanation of this rotation is related to the phase-conjugate nature of this diffraction order that forms a real image of the object. The other non-Bragg order image is angularly amplified due to the divergence of this diffraction order.
For this type of surface relief grating, it was shown that higher-order diffraction combines two self-diffracted waves [5]. Thus, it is possible to realize real-time interferometry with phase-shifting in all four diffracted beams. The intensity in each diffracted beam can be described by interferograms with phase shifts similar to those described by Eqs. (4-5).

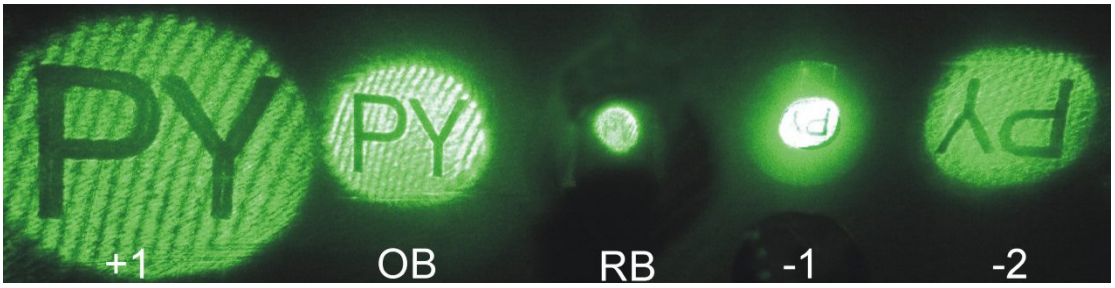
In the case of LN, we have phase-shifting interferometry realized in one exposure.
Figure 7a shows the imaging and interferometry from the metal reflective diffusion object, with letters PY (initial state) and after the rotation of the object around a vertical axis interference pattern (Figure 7b) in all diffracted orders. These results are similar to the experiments with lithium-niobate, where the phase-conjugated non-Bragg orders are rotated 180-degree around the vertical axis.




a)



Downloaded From: https://www.spiedigitallibrary.org/conference-proceedings-of-spie on 28 Nov 2023
Terms of Use: https://www.spiedigitallibrary.org/terms-of-use




b)

Figure 7. Imaging and interferometry: a) in Bragg (OB,RB) and in non-Bragg (+1,-1.+2) diffraction orders: initial state, b) object after deformation (rotation around vertical axis 15'')

During the reconstruction of the recorded hologram (when the object wave is blocked) the static deformations of the fine structures (of order of ~0,1mm) of the diffusion-reflected object can be revealed (Figure 8)

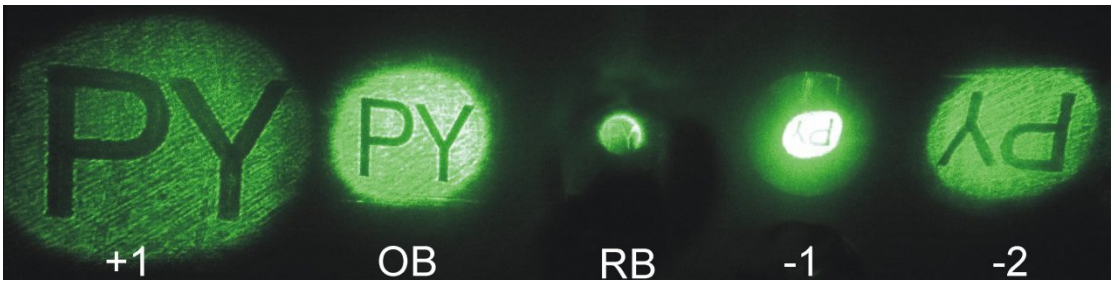



Figure 8 . A reconstruction of the recorded hologram of the diffusion reflection object (when object wave is blocked) that reveals the static deformation of the order of ~0,1mm.in non-Bragg orders.

In addition to the interferometric experiments, we have tested the ability of PTP materials for holographic recording and imaging via phase-distorting media [6,7]. In the optical schematic of Figure 5b, a grounded glass was placed between object and objective as a phase aberrator.



Downloaded From: https://www.spiedigitallibrary.org/conference-proceedings-of-spie on 28 Nov 2023
Terms of Use: https://www.spiedigitallibrary.org/terms-of-use

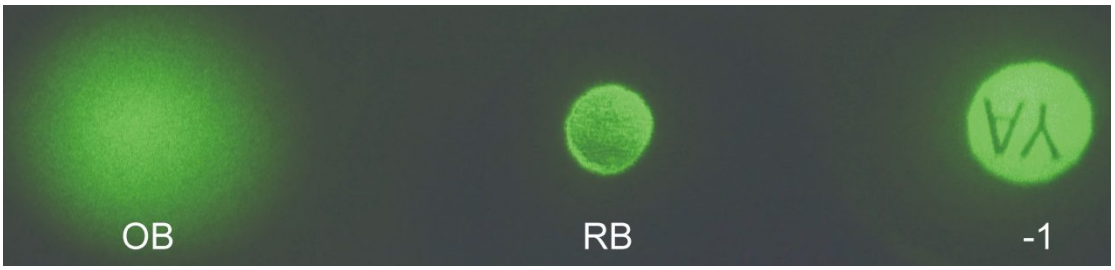



Figure 9. View of the holographic imaging through a phase aberrator. Left: direct imaging shows only a diffuse spot. Right: the image reconstructed in non-Bragg order after the hologram recording.

Direct imaging through an aberrator shows only a diffuse spot (left on the Figure 9), however, (Figure 9, right) shows the image after the hologram recording image is revealed in the the non-Bragg order

Another set of experiments was to check sensitivity of non-Bragg diffraction orders for retrieval with time-modulated object wave.Recording of grating was in a standard 2-beam geometry by HeNe laser with angle between beams ~ 5.73 deg., (or 0.1 rad, that gives period of grating as 6.14 microns), polarized in the plane of incidence (p-polarized) with grating vector along the C-axis of Fe-doped LN crystal (4 X 4 X 0.2 cm). Object wave was formed by the reflection from the piezoelectric plate, intensities of the reference and object waves are 24 mW and 6 mW respectively

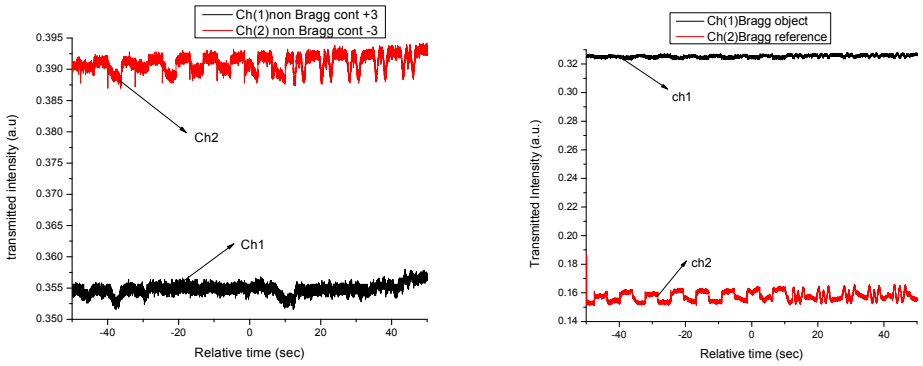



Fig.10. Intensities of Bragg (a) and non-Bragg (b) diffraction orders, when intermittently reference and signals waves are step-wise and saw-tooth modulated in time. It is seen, that highest sensitivity to displacement is in the -3 non-Bragg order (next to he reference beam) and in the reference beam.

## 4. CONCLUSIONS

Based on these results, we suggest the use of non-Bragg diffraction orders for imaging in both target rotation and angular amplification. In addition, it was demonstrated, that the PTP materials can achieve holographic recording and imaging through phase aberration with the image appearing in the non-Bragg diffraction order.

Retrieval of recorded hologram with a time-modulated object wave lead to time modulation of all diffracted orders (Bragg and non-Bragg), with higher sensitivity in non-Bragg diffraction orders.

Different types of materials, PTP-films and LN-crystals, and different types of gratings are shown to exhibit similar performance, producing higher-order diffracted beams. This one-shot (one-exposure) phase-shifting interferometry clarifies object wave-front information (as with the example of the surface deformation) and solves sign ambiguity problem.

Due to a high-resolution and the efficient imaging of the PTP -holographic camera static deformations in the order of ~0.1mm can be revealed on the diffusion reflection surface.



Downloaded From: https://www.spiedigitallibrary.org/conference-proceedings-of-spie on 28 Nov 2023
Terms of Use: https://www.spiedigitallibrary.org/terms-of-use

In addition, it was demonstrated that PTP materials can achieve holographic recording and imaging through phase aberration, with the image appearing in the non-Bragg diffraction order.

## ACKNOWLEDGMENTS

The authors thank the collaborators of the National Centre for Materials Study and Testing of Moldova Technical University for the opportunity to measure the deformation characteristics of thin films on their Atomic Force Microscope. The investigations performed in Moldova State University was financially supported by the Science and Technology Centre in Ukraine (STCU, Project Agreement Nr. 5404). The team from Alabama A&M University has been supported by Title III Program.

## REFERENCES

[1]. Volodin B. L Kippelen B., Meerholz K., Kukhtarev N. V., Caulfield H. J, Peyghambarian N., "Non-Bragg orders in dynamic self-diffraction on thick phase gratings in a photorefractive polymer", Opt. Lett**.,** *21*, 519-521( **199)**

[2]..Chirita A, "Real-time scaling of micro-objects by multiplexed holographic recording on photo-thermo-plastic structure", Journal of Modern Optics, *57*, 854 – 858 (**2010)**,

[3]..Credelle T, Spong, F., "Thermoplastic media for holographic recording", Holographic Recording Materials, Editor: H.Bjelkhagen, Proc SPIE, V. MS130, 619-633 (1996),

[4]. Golub M.A., Friesem A.A, Eisen. L., "Bragg properties of efficient surface relief gratings in the resonance domain", Optics Communications, *235, No.4-6*, 261-267**(2004)**,

[5]. Gaylord T.K.,.Moharam M.G, "Analysis and Application of Optical Diffraction by Gratings", Proceed. of IEEE, , *73,No.5*, 894-937 (**1985)**

[6]. Collier R. J. [Optical Holography], Academic Press, (1971).

[7]. Francon M., "Holographie", Masson et C, Paris, (1969).



Downloaded From: https://www.spiedigitallibrary.org/conference-proceedings-of-spie on 28 Nov 2023
Terms of Use: https://www.spiedigitallibrary.org/terms-of-use